Marfan Syndrome

22

Francesco Ramirez and Julie De Backer

Keywords
Dissecting aneurysm · Fibrillin 1 · Marfan syndrome · Mechanosensing · TGFβ signaling

22.1 Case Report

22.1.1 Family 1

At 2.5 years of age, the proband (III.3 in Fig. 22.1) was referred to an orthopedic surgeon for evaluation of pronounced flat feet with medial displacement of the medial malleolus. In addition to flat feet and tall and slender stature (105 cm, >p97, 11 kg < p10), a mild pectus carinatum deformity and marked generalized joint laxity were noted (Fig. 22.2). The orthopedic surgeon considered Marfan syndrome (MFS) in his differential diagnosis, and the boy was referred for cardiac evaluation where mild aortic root dilatation at the level of the sinuses of Valsalva (20 mm, z-score 2.8) and mitral valve prolapse (MVP) were diagnosed on cardiac ultrasound. Lens luxation was excluded on a slit lamp study. Based on these findings, a diagnosis of MFS was "suspected." Regular cardiac and orthopedic surveillance was scheduled.

The proband had two older brothers (Fig. 22.1), both tall, and one of them had some stretch marks, while the other one had mild myopia. Cardiac ultrasound in both of them was normal. Their parents' medical history was uneventful, but evaluation in the father revealed the presence of a chronic and complex type B aortic dissection, deemed unsuitable for repair at that time. He had a history of severe flat feet, being a reason for excluding him from military service. He didn't have any clinically significant scoliosis and presented a much milder pectus excavatum than his son. He had severe myopia since childhood. Beta-blocker treatment was initiated. Seventeen months after diagnosing the dissection, the proband's father died during surgery from acute aortic rupture of the dissected vessel at 45 years of age.

Due to excessive growth, the proband received testosterone treatment during puberty. Beta-blockers had not been given up to that point for reasons of mild asthma but were initiated with the testosterone treatment. With growth his scoliosis worsened to the extent of requiring surgical correction at 14 years of age (Fig. 22.3).

F. Ramirez (✉)
Department of Pharmacological Sciences, Icahn School of Medicine at Mount Sinai, New York, NY, USA
e-mail: francesco.ramirez@mssm.edu

J. De Backer
Department of Cardiology and Center for Medical Genetics, Ghent University Hospital, Ghent, Belgium
e-mail: Julie.DeBacker@ugent.be

© Springer Nature Singapore Pte Ltd. 2019

T. Oohashi et al. (eds.), *Human Pathobiochemistry*, https://doi.org/10.1007/978-981-13-2977-7_22

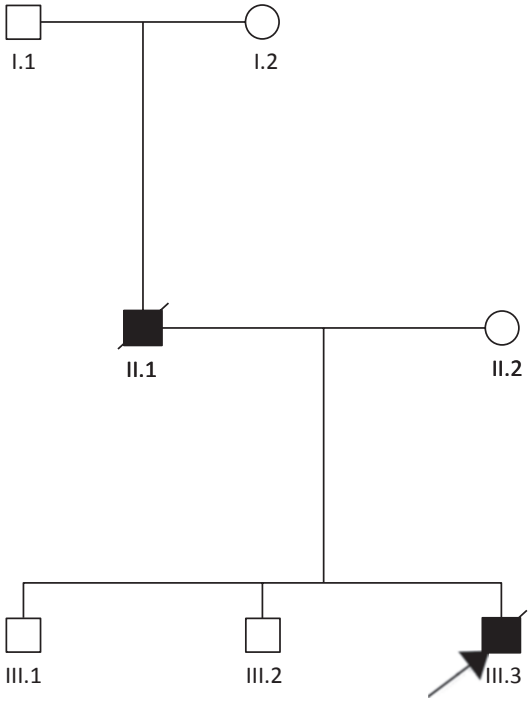

Fig. 22.1 Pedigree of Family 1 (F1). Proband (III.3) is indicated with an arrow; square symbols represent males, circles females; black symbols indicate affected individuals

Clinically, the boy developed additional characteristic skeletal manifestations, including marked pectus carinatum, arachnodactyly, decreased elbow extension, and distinctive facial features with downslanting palpebral fissures, malar hypoplasia, and a high-arched palate. His height at the age of 14 was 184 cm and weight 49 kg. Cardiac ultrasound revealed progressive dilatation of the aortic root at the level of the sinus of Valsalva (47 mm; z-score 6.8 at age 14–52 mm at age 15 and 56 mm at age 15.5) as well as mitral valve prolapse with mild mitral valve regurgitation.

Two years after scoliosis surgery, the proband underwent elective valve-sparing aortic root replacement. The surgical procedure was complicated by an episode of ventricular fibrillation requiring DC shock. After surgery, the proband developed left ventricular dilatation. A coronary angiography performed 10 months after surgery revealed normal coronary arteries. On follow-up at the age of 19, progressive dilatation with markedly depressed left ventricular systolic function was noted with a left ventricular end-diastolic diameter of 81 mm (normal 50 ± 4.1 mm) and an ejection fraction of 25% (normal 62%).

At the age of 24, the proband collapsed while driving his car and died. Autopsy revealed the absence of aortic dissection and no intracerebral abnormalities – sudden arrhythmic cardiac death was suspected as the cause of death. Genetic testing performed shortly before his death had revealed the presence of a mutation in the fibrillin-1(*FBN1*) gene (c.305_306del insAA; p.Cys102X in exon 3), which was not found in both of his brothers and his paternal grandparents.

22.1.2 Family 2

Cardiovascular evaluation for palpitations in the 62-year-old male proband in the second family (F2-II.1 in Fig. 22.4) revealed an aneurysm of the ascending aorta. The man had normal blood pressure, never smoked and had normal serum cholesterol levels. The diameter of the aortic root at the level of the sinuses of Valsalva was 57 mm (z-score 6.2). He underwent aortic root replacement using a composite graft (Bentall procedure with replacement of the proximal aorta by a Dacron graft and replacement of the aortic valve with a mechanical prosthesis). After surgery, the patient was referred to the medical genetics department for diagnostic work-up.

Medical history revealed that he had undergone ocular surgery at the age of 47 for bilateral cataract and 5 years later for glaucoma. Ocular examinations prior to these interventions had identified microspherophakia and very shallow anterior eye chambers, reminiscent for ocular features of Weill-Marchesani syndrome (WMS). On physical examination, the proband presented a stocky build with a height of 173 cm and weight of 110 kg (Fig. 22.5). His arm span-to-height ratio was greater than normal (armspan 183 cm, ratio 1.06, normal <1.05), but the upper/lower segment ratio was normal (0.92). He had a round face and a characteristically flat skull (brachycephaly). He presented marked stiffness of the

Fig. 22.2 Images of the proband in Family 1 as a child; his father is shown in the picture on the left

finger joints and brachydactylia. The chest wall, spine, elbows, and feet were all normal on inspection. He had no stretch marks.

The proband's family history revealed that his older brother and sister had a very similar phenotypic appearance. Reportedly, they both had ocular problems and had died suddenly at the age of 63 and 45, respectively. The proband's mother and maternal uncle also had been diagnosed with glaucoma. However, they were tall and had long, slender fingers. They both died suddenly at the age of 84 and 70, respectively, from an "unspecified cardiac cause."

Based on the presence of a thoracic aortic aneurysm with a family history of sudden death, the proband was tested for a probable *FBN1* mutation. A heterozygous 12 nucleotide in frame deletion was detected in exon 20 of the *FBN1* gene (c.2502-2513delT- GAAAGTACTTT; p.Glu 835-Leu838del). It was not until the identification of the genetic defect that the proband agreed to contact and examine his children. Physical examination of the eldest son (F2-III.1) revealed the presence of mild skeletal features of MFS (increased armspan, arachnodactylia), in addition to severe myopia, bilateral upward luxation of the lenses, and moderate dilatation of the proximal aorta at the level of the sinuses of Valsalva (43 mm, z-score 3.14). Examination of the proband's 7-year-old grandson (F2-IV.2) revealed several skeletal manifestations, including scoliosis, pectus deformity, arachnodactylia, and flat feet, as well as bilateral subluxation of the lenses and myopia. Echocardiographic evaluation was completely normal at that time. Molecular studies confirmed the presence of the *FBN1* deletion in the proband's son and grandson. Clinical evaluation of the proband's daughter (F2-III.4) showed no manifestations of MFS. Molecular analysis confirmed the absence of the *FBN1* mutation. The proband's granddaughter (F2-IV.1) was only evaluated molecularly and found not to carry the *FBN1* mutation. Over the years, the proband's grandson (F2-IV.2) developed progressive aortic root dilatation, which by the age of 16 had a diameter of 41 mm

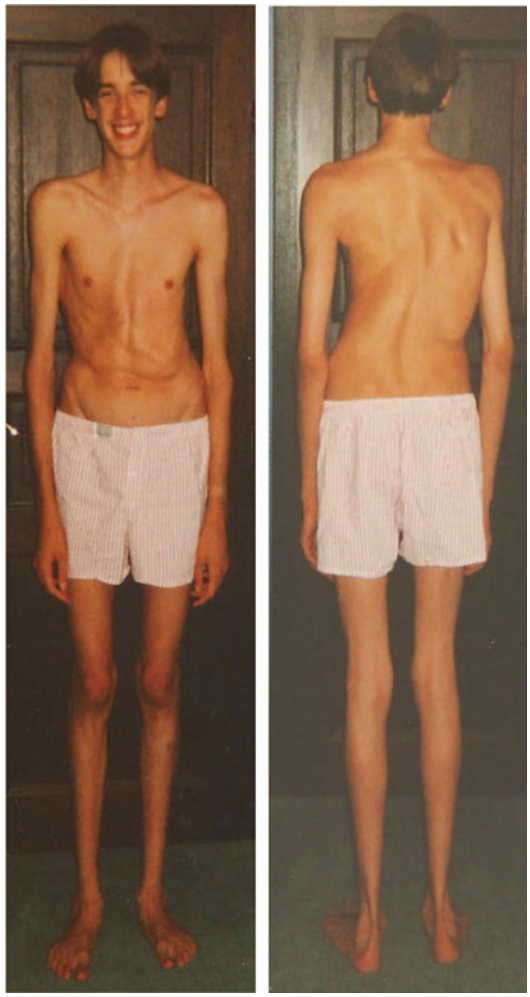

Fig. 22.3 Images of the proband in Family 1 at age 14 prior to scoliosis surgery

(z-score 4.8) at the level of the sinus of Valsalva – on the other hand, his father showed no additional growth of the aneurysm, remaining stable at 43 mm.

22.2 Diagnosis: Marfan Syndrome (MFS)

The first clinical description of MFS was at the end of the nineteenth century by the French pediatrician Antoine Bernard Marfan, who reported of a young girl presenting a combination of striking skeletal features. However, it is now well-established that the skeletal manifestations of MFS are not specific to this disease condition but show significant overlap with other connective tissue disorders and other genetic aortic disease entities (Table 22.1).

Many skeletal features of MFS can also occur in the general population, and conversely many MFS patients may not exhibit the full phenotype. As a result, MFS diagnosis relies on strict clinical criteria that have evolved over time. The current MFS nosology (aka, revised Ghent nosology; Loeys et al. 2010a) stipulates that diagnosis requires the presence of two cardinal clinical features (aortic root dilatation and ectopia lentis) and a systemic score based on manifestations in different organ systems. Depending on family history, seven diagnostic scenarios based on cardinal features are possible:

In the absence of family history:

1. Ao ($Z \geq 2$) + EL = MFS
2. Ao ($Z \geq 2$) + *FBN1* = MFS
3. Ao ($Z \geq 2$) + Syst (≥7 pts) = MFS
4. EL + *FBN1* with known Ao = MFS

In the presence of family history:

5. EL + FH of MFS (as defined above) = MFS
6. Syst (≥7 pts) + FH of MFS (as defined above) = MFS
7. Ao ($Z \geq 2$ in adults, $Z \geq 3$ in children) + FH of MFS (as defined above) = MFS

Ao aortic root dilatation defined as a z-score ≥2 for adults and ≥3 for children; *EL* ectopia lentis; *Syst* systemic score. "Adults" are defined when ≥20 years.

Systemic features used for MFS diagnosis are scored as follows:

Wrist and thumb sign **– 3** (wrist or thumb sign – **1**)
Pectus carinatum deformity **– 2** (pectus excavatum or chest asymmetry – **1**)
Hindfoot deformity **– 2** (plain pes planus – **1**)
Protrusio acetabuli **– 2**
Pneumothorax **– 2**
Dural ectasia **– 2**

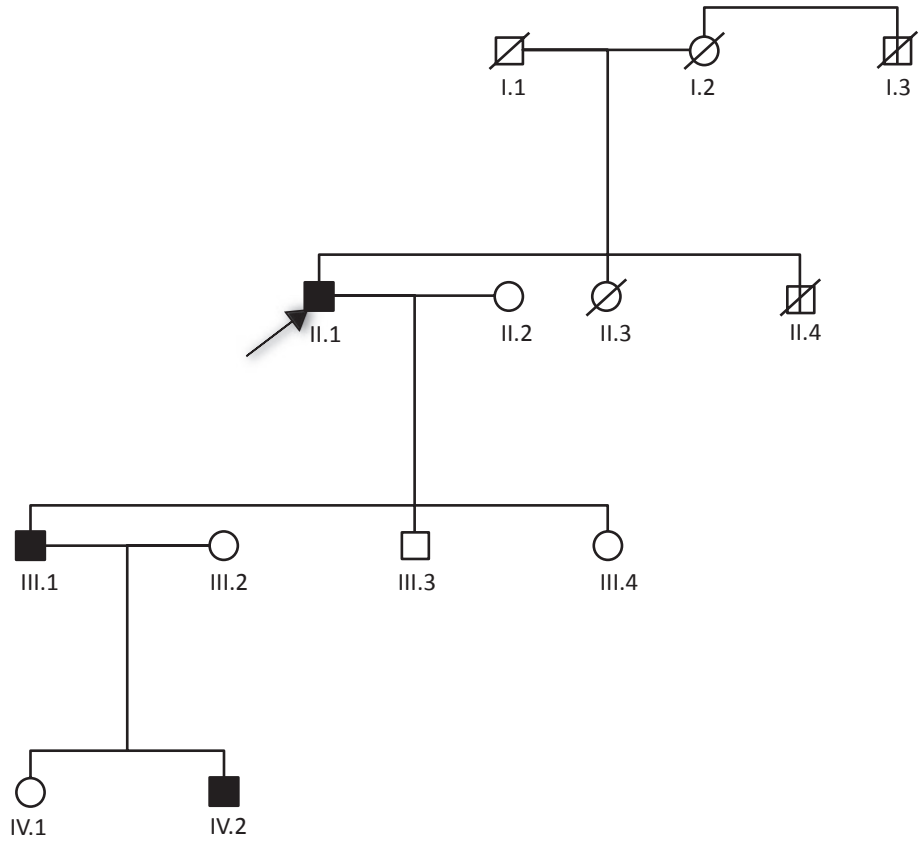

Fig. 22.4 Pedigree of Family 2; the proband (II.1) is indicated with an arrow

Reduced US/LS and increased arm/height and no severe scoliosis **– 1**
Scoliosis or thoracolumbar kyphosis **– 1**
Reduced elbow extension **– 1**
Facial features (3/5) **– 1**
Skin striae **– 1**
Myopia >3 diopters **– 1**
Mitral valve prolapse (all types) **– 1**
TOTAL: 20 points

While improved, MFS diagnosis can still be a challenge particularly in young children who have not yet developed the full-blown phenotype. In these cases, intermediate diagnoses like "non-specific connective tissue disorder" and "potential MFS" can be used. Several issues related to the diagnostic difficulties in MFS are nicely illustrated by the cases presented above:

1. At the initial evaluation at 2.5 years of age, the boy of the first family did not fulfill the diagnostic criteria of MFS. With a systemic score of 5/20, an aortic root z-score of 2.8, and no ectopia lentis, he would have been classified as afflicted with a "non-specific connective tissue disorder."
2. As illustrated by the proband of Family 2 and the boy's father of F1, outward features of the disease may be absent or so subtle to go unnoticed throughout life – often until a fatal event occurs.
3. The variability of clinical features in patients with MFS may be striking, even within the same family. Case in point is the very pronounced skeletal abnormalities of the proband in Family 1 that were largely absent in his father. The variability in the second family is

Fig. 22.5 Image of the proband in Family 2

even more striking and does not only apply to the skeletal system but also to the ocular and cardiovascular system.

4. Molecular testing is helpful for the diagnosis of affected family members *and* for exclusion of the diagnosis in unaffected family members. Both brothers of the proband in Family 1 had mild Marfanoid features – demonstrating the absence of the molecular defect was extremely important for reassuring them and their mother who had lost both her husband and son.

22.2.1 Thoracic Aortic Disease (TAD)

As already mentioned, aortic root dilatation in MFS is one of the cardinal features in the diagnostic setting and is the most important factor determining life expectancy. The diagnosis of aortic root dilatation requires careful measurement of the aortic diameter at the correct location and according to standardized methods. In MFS, the dilatation typically occurs at the level of the sinuses of Valsalva. Obtained values need to be corrected for the individual's age, gender, and body surface area (Devereux et al. 2012). Commonly, z-scores are calculated, taking into account the obtained and expected diameter for a specific individual: z-score = (obtained diameter – expected diameter)/standard deviation. A z-score is a measure of how many standard deviations below or above the population mean a raw score is – as such a z-score >2 indicates that the value obtained for that individual exceeds 2 standard deviations of what is expected.

While the technical details of aortic root z-score calculation are beyond the scope of this chapter, some points are nonetheless worthwhile to be mentioned: (1) the method used to calculate the z-score should be exactly the same as the one used to generate the reference values used in the calculation – methodological aspects such as imaging technique and location and timing of the measurement are critical; (2) the reference population should match and cover the age range of the patient; (3) assessment of aneurysm progression in the same patient can vary as the patient grows or gains or loses weight.

Similar to skeletal manifestations, aortic root dilatation alone is not diagnostic for MFS, and patients with a dilatation of the aortic root need to be carefully evaluated in order to define the underlying cause. In older patients, as in the proband of the second family, atherosclerosis commonly underlies aortic aneurysm formation, and assessment of conventional cardiovascular risk factors is important. Additionally, careful clinical evaluation of the proband, supplemented by a dedicated ocular exam, is mandatory. Last but not least, a detailed family history and clinical assessment of first-degree relatives in selected cases are necessary to confirm diagnosis.

The cases presented here nicely illustrate the importance of assessment of family members. Diagnosis in the young boy in Family 1 was uncertain, but assessment of his father further raised suspicion of MFS, even though he did not fulfill the diagnostic criteria. In the second case, the diagnosis in the proband could have been confirmed with assessment of his son, underscoring the increasing importance of molecular genetic testing. Based on clinical evaluation and family history in the proband, an underlying

Table 22.1 Skeletal features in MFS and related diseases

Skeletal features in MFS	Arachnodactylia, increased armspan, decreased upper to lower segment ratio, decreased elbow extension, pectus deformities, kyphoscoliosis, flat feet, protrusio acetabuli, facial characteristics	
Skeletal features in other connective tissue and genetic aortic disorders		
	Features in common with MFS	Discriminating features – not typical for MFS
Congenital contractural arachnodactyly	Arachnodactylia, pectus deformities, decreased elbow extension, scoliosis	Joint contractures of the hips and knees, crumpled ears, clinodactyly
Kyphoscoliotic Ehlers-Danlos syndrome	Kyphoscoliosis	Skin features
Homocystinuria	Tall stature, increased armspan	Developmental delay/ intellectual disability
Loeys-Dietz spectrum	Pectus deformities, scoliosis, arachnodactylia	Hypertelorism, split uvula, club feet

genetic entity may be suspected – in this respect both syndromic and non-syndromic forms are recognized. Identified genetic aortic entities, grouped under the denominator heritable thoracic aortic disease (H-TAD), are listed in Table 22.2 along with their respective genetic and clinical features (Pyeritz 2014).

MFS is the prototypical syndromic H-TAD. Other forms of syndromic H-TAD include Loeys-Dietz syndrome (caused by mutations in components of the TGFβ signaling pathway; Loeys et al. 2006), aneurysm-osteoarthritis syndrome (caused by mutations in *SMAD3*, an intracellular component of the TGFβ signaling pathway; van de Laar et al. 2011), and smooth muscle cell dysplasia syndrome (caused by the R179 mutation in *ACTA2*; Milewicz et al. 2010). Differentiating these syndromes is often difficult due to overlapping manifestations; similar considerations apply to non-syndromic forms of H-TAD. However, identifying the underlying mutation in H-TAD may be helpful in risk stratification and management of individual patients. Arterial disease in MFS vs. Loeys-Dietz syndrome best exemplifies this point. Whereas patients harboring mutations in *FBN1* generally have a lower risk for developing aortic dissection at diameters below 55 mm, those with mutations genes involved in the TGFβ pathway generally evolve more aggressively and require earlier surgery (Milewicz and Regalado 2015).

22.2.2 Other Cardiovascular Manifestations

With extended life expectancy thanks to improved treatment and management of aortic disease, an increasing amount of MFS patients develop aneurysms elsewhere in the arterial tree. Apart from increasing diameters, the aorta also elongates with age, which forces the anatomically fixed aorta to bend and become tortuous. By means of magnetic resonance imaging (MRI), the tortuosity index can be measured and used as a marker of aortic disease severity in MFS.

MVP is an established clinical feature of MFS that occurs in >60% of cases. MVP is often a reason for referral in young children and shows a less benign course in MFS patients than in the general population (Judge and Dietz 2005). MFS-related cardiomyopathy is subclinical in most cases although severe forms – even necessitating cardiac transplantation – have been reported. Indeed, heart failure resulting from cardiomyopathy has been reported as the main cause of death in both surgical and clinical follow-up data in MFS series. Underlying valvular heart disease may cause dilated cardiomyopathy (DCM) in MFS, but there is also experimental evidence for intrinsic myocardial dysfunction. Clinical evidence that left ventricular contractility and ventricular-vascular coupling are abnormal in MFS, independent of aortic stiffness, is

Table 22.2 Overview of clinical entities to be taken into account in the differential diagnosis of H-TAD (both syndromic and non-syndromic). Distinctive cardiovascular and other clinical features are indicated in bold

Disorder	Gene(s)	Main cardiovascular features	Additional clinical features
Syndromic H-TAD			
Marfan	*FBN1*, *TGFBR1&2*	**Sinus of Valsalva aneurysm**, aortic dissection, mitral valve prolapse, main pulmonary artery dilatation, left ventricular dysfunction	**Lens luxation**, skeletal features (arachnodactylia, pectus deformity, scoliosis, flat feet, increased armspan, dolichocephalia), dural ectasia, striae
	SMAD3, *TGFB2*		
Loeys-Dietz	*TGFBR1&2*	**Sinus of Valsalva aneurysm**, aortic dissection, arterial aneurysms and dissections, **arterial tortuosity**, patent ductus arteriosus, atrial septal defect, bicuspid aortic valve	**Bifid uvula/cleft palate**, **hypertelorism**, pectus abnormalities, scoliosis, club feet
	SMAD3, *TGFB2&3*		
Vascular Ehlers-Danlos syndrome	*COL3A1*	**Arterial rupture and dissection without preceding dilatation/aneurysm**	**Gastrointestinal rupture**, **thin and translucent skin**, dystrophic scars, facial characteristics (Madonna face, thin lips, deep set eyes), club feet, uterine rupture
Multi-systemic smooth muscle dysfunction syndrome	*ACTA2*	**Ascending aortic aneurysm**, aortic dissection, **patent ductus arteriosus**, aortic coarctation, aortopulmonary window, pulmonary arterial hypertension	**Congenital mydriasis**, malrotation of the gut, moyamoya disease, periventricular white matter hyperintensities
Shprintzen-Goldberg syndrome	*SKI*	**Mild aortic root dilatation**, mitral valve prolapse	**Craniosynostosis**, distinctive craniofacial features, skeletal changes, neurologic abnormalities, mild-to-moderate intellectual disability
Arterial tortuosity syndrome	*SLC2A10*	**Arterial tortuosity**, arterial stenoses and aneurysms, mild aortic root dilatation	Hyperlax skin and joints, beaked nose, elongated face, micrognatia
Cutis laxa syndromes (autosomal dominant and recessive)	*ELN*, *FBLN4*	Mild aortic dilatation and tortuosity	Skin hyperlaxity, emphysema, downslanting palpebral fissures, inguinal hernia
Non-syndromic H-TAD			
	ACTA2	Thoracic aortic aneurysm/ dissection, cerebrovascular disease, coronary artery disease	Lack of Marfanoid skeletal features, **livedo reticularis**, **iris flocculi**, **coronary artery/ cerebrovascular disease**
	TGFBR1/2	Thoracic aortic aneurysm/ dissection	Lack of syndromal features
	FBN1	Sinus Valsalva aneurysm, mitral valve prolapse	**Lack of syndromal features**
	MYLK	Thoracic aortic aneurysm/ dissections often at low aortic diameters	
	SMAD3	Intracranial and other arterial/ visceral aneurysms	
	TGFB2	**Mitral valve prolapse**	
	MYH11	**Patent ductus arteriosus**	
	PRKG1	**Aortic dissection at young age**	
	MFAP5	**Lone atrial fibrillation**	

also consistent with intrinsic impairment of myocardial contractility. Probably related to both MVP and cardiomyopathy are cardiac arrhythmias and increased ventricular ectopia. As discussed in the next section, the emerging view is that structural abnormalities altering mechanosignaling underlie myocardial dysfunction in MFS.

While it is obvious that MFS and nonsyndromic H-TAD are part of one clinical spectrum, it is more difficult to reconcile how mutations in *FBN1* can also cause acromelic dysplasias, which manifest short stature, short hands and feet, stiff joints, and a hypermuscular build – in other words the opposite phenotype than MFS. Geleophysic dysplasia, acromicric dysplasia, and WMS are all part of the acromelic dysplasia group of diseases, and they can all be associated with rare mutations in *FBN1*.

22.3 Molecular Perspectives

Mutations that impair the structure or reduce the expression of the extracellular matrix (ECM) protein fibrillin-1 are responsible for the multisystem manifestations of MFS. Fibrillin-1 is an ubiquitous 350-kD glycoprotein made almost entirely of calcium-binding EGF (cb-EGF) repeats interspersed with a few 8-cysteine (TB/8-Cys) motifs (Fig. 22.6a; Sakai et al. 2016). Calcium binding stabilizes contiguous cb-EGF sequences into a rigid linear structure required for fibrillin-1 polymerization, interaction with other matrix proteins, and protection from proteolytic enzymes. Aside from fibrillin-1 and the structurally related fibrillin-2, TB/8-Cys modules are only found in latent TGFβ-binding proteins (LTBPs), key regulators of TGFβ bioavailability. LTBPs bind the dimeric pro-peptide of TGFβ non-covalently associated with the bioactive ligand (aka, small latent complex or SLC) so as to facilitate folding and secretion of the resulting tripartite complex (aka, large latent complex or LLC), which is then tethered to the ECM in part via LTBP association with fibrillin-1 assemblies (microfibrils and elastic fibers) (Fig. 22.6b; Robertson and Rifkin 2016).

Fibrillin-1 microfibrils are assembled through an undefined hierarchical process whereby individual molecules are organized into head-to-tail polymers that associate laterally with one another and incorporate other ECM proteins within them (Fig. 22.6a). Fibrillin-1 microfibrils can also serve as the scaffold guiding tropoelastin alignment and cross-linking in the elastic fibers (Fig. 22.6a). Fibrillin-1 assemblies therefore represent a unique example of a dual-function component of the architectural matrix. The first role is structural in that they endow tissues with tensile strength and elasticity, in addition to demarcating functionally distinct areas within them; the second role is instructive for they modulate the behavior of resident cells by interacting with integrin receptors and LLCs. TGFβ sequestration into the ECM promotes spatial distribution and proper concentration of bioactive ligands for either immediate presentation to cells or subsequent release during tissue remodeling/repair (Fig. 22.6b). All *FBN1* mutations translate into MFS tissues with less fibrillin-1 immunostaining as a result of impaired mRNA stability, reduced protein secretion, or/and increased protein degradation. While the mechanistic relationship between *FBN1* mutations and MFS severity remains largely undefined, studies of mice with genetically engineered *Fbn1* mutations have yielded insights into organ-specific disease processes. Examples relevant to cardiovascular manifestations in MFS are described below along with current speculations about how some domain-specific mutations in fibrillin-1 may cause non-MFS phenotypes.

22.3.1 TAD

Aortic aneurysms are characterized by progressive vessel dilation associated with smooth muscle cell (SMC) dysfunction, localized inflammatory infiltrates, and destructive (maladaptive) ECM remodeling that, together, predispose the arterial wall to tear (dissection) and rupture. Consistent with the degenerative nature of the disease, inherited forms of TAD are accounted for by mutations in molecules nor-

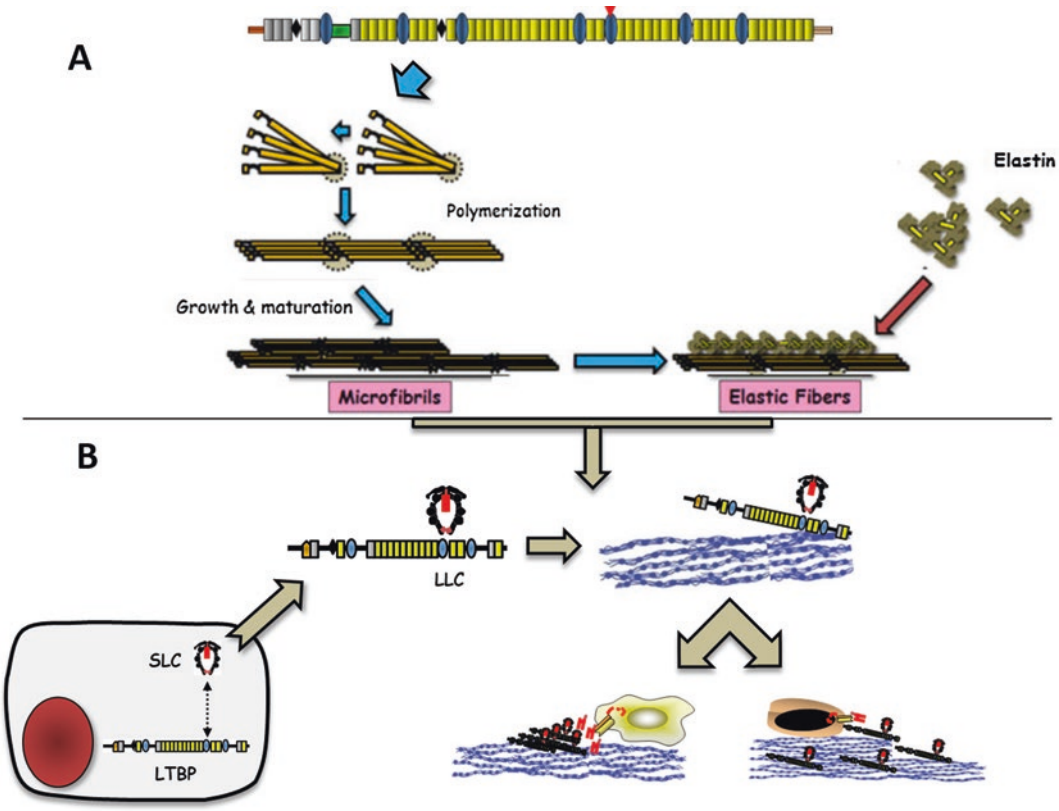

Fig. 22.6 Fibrillin microfibrils' biogenesis (**a**) and interaction with TGFβ complexes (**b**). At the top of Panel A is shown the primary structure of fibrillin-1 protein with yellow rectangles, blue ovals, and red triangle representing EGF-cb and TB/8-Cys motifs and RGD integrin-binding site, respectively. At the bottom right of Panel B are depicted how fibrillin-1 assemblies promote spatial distribution and proper concentration of bioactive ligands for either immediate presentation to cells or subsequent release during tissue remodeling/repair

mally implicated in supporting tissue integrity and homeostasis, such as components of the ECM, SMC cytoskeleton, and TGFβ signaling pathways (Milewicz et al. 2017). In this respect, MFS represents an informative model to characterize altered cell-matrix interactions leading to progressive degeneration and ultimately, structural collapse of the aortic wall. Fibrillin-1 assemblies are abundantly distributed throughout the vessel wall, as components of the elastic lamina underneath endothelial cells in the intima, as sheets of interconnected elastic fibers that together with concentric layers of SMCs constitute the contractile unit of the media, and as the loosely arranged meshwork intermixed with collagen fibrils that engulfs fibroblasts, nerve, and stem cells in the adventitia (Wagenseil and Mecham 2009).

In spite of significant research effort, the molecular mechanism of arterial disease in MFS remains controversial with negative implications for developing new evidence-based drug treatments. The major controversy centers on TGFβ's role in TAD pathogenesis and the mechanistic relationship between TGFβ over-activation and constitutively elevated signaling by the angiotensin II (AngII) type I receptor (AT1R) (Chen et al. 2013). Earlier studies with MFS mice manifesting TAD without dissection and rupture had concluded that AT1R-dependent TGFβ hyperactivity is the main driver of TAD development and, consequently, that AT1R antagonism may prevent

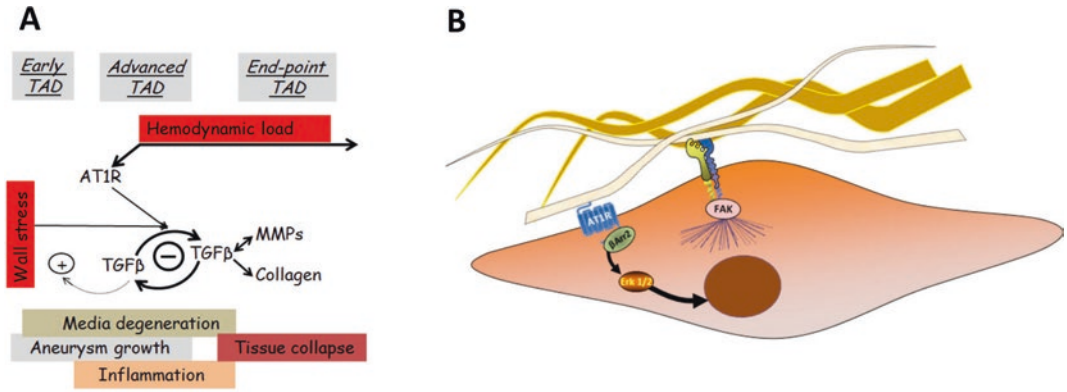

Fig. 22.7 Proposed models of aortic aneurysm (**a**) and cardiomyopathy (**b**) in MFS that are both based on findings from studies of mouse models of the disease (Cook et al. 2014, 2015)

TAD formation by blunting TGFβ signaling (Habashi et al. 2006). However, subsequent studies have shown partially overlapping roles of AT1R and TGFβ hyperactivity in driving TAD formation and progression, respectively, in addition to revealing a protective (AT1R-independent) role of baseline TGFβ signaling during postnatal vessel growth (Li et al. 2014; Cook et al. 2015) Accordingly, an alternative new model of TAD pathogenesis has emerged whereby a fibrillin-1-deficient aortic matrix communicates to resident cells signals of hemodynamic load and wall stress that are translated into biochemical responses aimed at maintaining physiological tone (Fig. 22.7a). Among others, the model predicts that the early response of the MFS aorta to physiological blood pressure increase includes AT1R over-activation and protective baseline TGFβ signaling whose effectiveness is impaired by fibrillin-1 deficiency. The model also predicts that dysregulated AT1R signaling, together with other wall stress-induced processes, such as inflammation and ECM remodeling, gradually establishes an irreversible TGFβ-centered loop that drives media degeneration ultimately leading to physical collapse of the vessel wall. Implicitly, this new disease model argues for a combinatorial drug treatment strategy that would target promiscuous AT1R and TGFβ signaling while sparing the early protective role of TGFβ activity.

22.3.2 DCM

Heart function largely depends on the ECM ability to transmit mechanical forces to cardiomyocytes where mechanosensors, including AT1R and ECM-binding integrins, convert stretch stimuli into biochemical signals that regulate muscle activity to maintain tissue homeostasis. Cardiomyocytes can also adapt to elevated workload by augmenting contractility and increasing their mass (hypertrophy) so as to normalize cardiac output. Genetic lesions or environmental insults that interfere with this physiological response lead to maladaptive tissue remodeling and cardiomyopathy. Cardiac valve disease and stiffening of the dilating aortic wall have long believed to cause heart dysfunction in MFS by imposing volume overload on the left ventricle. However, subsequent analyses of mice with tissue-specific inactivation of the *Fbn1* gene expression have refuted this notion by demonstrating that fibrillin-1 deficiency in the myocardium is necessary and sufficient to trigger DCM (Cook et al. 2014).

The myocardial matrix consists of highly specialized multi-protein structures that surround individual myocytes and interconnect them into a synchronously functioning unit. Fibrillin-1 microfibrils couple myocytes to the ECM, as associated components of basement membranes;

contribute to the mechanical properties of myocardial tissue, as obligatory constituents of interstitial elastic fibers; and weave together adjoining myocytes, as molecular bridges between macromolecular assemblies in the pericellular and interstitial matrices. In line with the structural integration of these fibrillin-1 assemblies into a single functional unit, fibrillin-1 deficiency significantly weakens the physical properties of the myocardium of MFS mice, and this in turn translates into impaired muscle contractility associated with abnormal myocyte mechanosignaling, as evidenced by AngII-independent AT1R hyperactivity and abated FAK-mediated integrin signaling (Fig. 22.7b). In contrast to TAD, TGFβ hyperactivity appears not to be involved in DCM formation. Consistent with these findings, systemic administration of losartan, an AT1R blocker, prevented DCM formation in MFS mice. Additionally, this drug treatment was also reported to mitigate ventricular dysfunction in MFS patients (Hartog et al. 2016).

22.3.3 MFS-Related Diseases

As already noted, the complex phenotype of the MFS/WMS family described in this chapter further underscores our limited understanding of genotype-phenotype relationships in MFS and related disorders, as well as of the role that genetic modifiers play in these different pathological correlates. This problem is particularly evident for the rare mutations in *FBN1* that have been associated with acromelic dysplasias, which manifest musculoskeletal abnormalities opposite of those normally seen in MFS (Sakai et al. 2016). The same consideration applies for mutations in *FBN1* that cause the tissue-specific phenotype of stiff skin syndrome (SSS; Loeys et al. 2010b). Unlike MFS mutations, which are spread throughout the entire fibrillin-1 molecule, those associated with acromelic dysplasias and SSS are clustered in domains believed to mediate interactions with cells and other matrix proteins. Indeed, experimental findings indicate that *FBN1* mutations causing acromelic dysplasias or SSS do not apparently affect the assembly or stability of fibrillin-1 microfibrils and that acromelic dysplasias can also be caused by mutations in molecules known to interact with fibrillin-1, such as LTBP3 and ADAMTSL2 (Sakai et al. 2016). However, this evidence does not explain how deletion of exon 20 would account for the variable phenotype of MFS/WMS family described here.

22.4 Treatment

We will limit our description to the treatment of cardiovascular abnormalities in MFS. It goes without saying that patients afflicted with this pleiotropic disorder require a multidisciplinary approach and appropriate treatment of major skeletal and ocular manifestations.

22.4.1 Medical Treatment

Slowing down aortic root growth rate and preventing dissection are the mainstays of treatment in patients with MFS. The most commonly prescribed drugs to achieve this are β-adrenergic blockers, which reduce the aortic dilation rate in patients with MFS due to their effects on aortic wall shear stress. Losartan, an AT1R blocker, might be an alternative or complementary therapy to β-blockers, since losartan reduces arterial pressure and potentially interferes with the pathophysiology of MFS by TGF-β antagonism. After evidence of losartan effectiveness in a mouse model of MFS (Habashi et al. 2006), several randomized clinical trials were launched to test losartan in various protocols. Despite the differences in study design and outcome, these studies consistently showed that losartan is not more effective in reducing the rate of aortic dilatation than a high dosage of β-blockers. Losartan may be regarded as a valid alternative in those patients that do not tolerate β-blockers, and hopefully, an ongoing large-scale meta-analysis will shed more light on possible subgroups that

may benefit from specific treatments (Pitcher et al. 2015).

22.4.2 Surgical Treatment

The threshold aortic diameter for prophylactic surgery in MFS is 50 mm at any level of the vessel or 45 mm at the aortic root. Associated risk factors include family history of dissection, progressive dilation of more than 2 mm/year, severe aortic or mitral valve regurgitation, or pregnancy. Over the past 30 years, the composite replacement of the aortic valve and ascending aorta (aka, "Bentall procedure") has proved to be low risk and very durable operation for aortic root aneurysm in MFS. Valve-sparing operations with root replacement by a Dacron prosthesis and reimplantation of the coronary arteries into the prosthesis (aka, the "David procedure") have now become the preferred choice due to the inherent need for lifelong anticoagulation after a Bentall procedure.

Treatment of aneurysms/dissections in the distal aorta of MFS patients also consists of medical treatment in a first step and surgery with documented increased growth rate or organ ischemia. Due to an increased rate of stent-related complications, open surgery is the preferred method for treatment. Techniques have evolved significantly over the last decades, mainly aimed at avoiding organ damage during the procedure. The father of the proband in the first family described here was considered too high risk for surgery 25 years ago, but today he might have undergone surgery.

MVP with significant valvular regurgitation is another reason for primary surgery in approximately 15% of MFS patients. Forty-five percent of cases will also undergo aortic root surgery at that time. About 20% of MFS patients undergoing aortic root surgery will simultaneously undergo a mitral valve procedure. Technically, mitral valve repair is associated with better survival than mitral valve replacement. Heart failure in MFS patients should be treated according to conventional guidelines and should include heart transplantation when indicated.

End of Chapter Questions

1. Molecular genetic testing may be useful in some situations to confirm the diagnosis in MFS – can you give an example?
2. How would you link the various genes identified in H-TAD patients?
3. What are possible targets for treatment in MFS?
4. What are the major mechanisms responsible for TAD and DCM development in mouse models of MFS?
5. Which connective tissue diseases are associated with *FBN1* mutations?

References

Chen X et al (2013) Conundrum of angiotensin II and TGF-β interactions in aortic aneurysms. Curr Opin Pharmacol 13:180–185

Cook JR et al (2014) Abnormal muscle mechanosignaling triggers cardiomyopathy in mice with Marfan syndrome. J Clin Invest 124:1329–1339

Cook JR et al (2015) Dimorphic effects of TGFβ signaling during aortic aneurysm progression in mice suggest a combinatorial therapy for Marfan syndrome. Arterioscler Thromb Vasc Biol 35:911–917

den Hartog AW et al (2016) The effect of losartan therapy on ventricular function in Marfan patients with haploinsufficient or dominant negative FBN1 mutations. Neth Hear J 24:675–681

Devereux RB et al (2012) Normal limits in relation to age, body size and gender of two-dimensional echocardiographic aortic root dimensions in persons ≥15 years of age. Am J Cardiol 110:1189–1194

Habashi JP et al (2006) Losartan, an AT1 antagonist, prevents aortic aneurysm in a mouse model of Marfan syndrome. Science 312:117–121

Judge DP, Dietz HC (2005) Marfan's syndrome. Lancet 366:1965–1976

Li W et al (2014) Tgfbr2 disruption in postnatal smooth muscle impairs aortic wall homeostasis. J Clin Invest 124:755–767

Loeys BL et al (2006) Aneurysm syndromes caused by mutations in the TGF-b receptor. N Engl J Med 355:788–798

Loeys BL et al (2010a) The revised Ghent nosology for the Marfan syndrome. J Med Genet 47:476–485

Loeys BL et al (2010b) Mutations in fibrillin-1 cause congenital scleroderma: stiff skin syndrome. Sci Transl Med 2:23ra20

Milewicz DM, Regalado ES (2015) Use of genetics for personalized management of heritable thoracic aortic disease: how do we get there? J Thorac Cardiovasc Surg 149:S3–S5

Milewicz DM et al (2010) De novo ACTA2 mutation causes a novel syndrome of multisystemic smooth muscle dysfunction. Am J Med Genet A 152A:2437–2443

Milewicz DM et al (2017) Altered smooth muscle cell force generation as a driver of thoracic aortic aneurysm and dissections. Arterioscler Thromb Vasc Biol 37:26–34

Pitcher A et al (2015) Design and rationale of a prospective, collaborative meta-analysis of all randomized controlled trials of angiotensin receptor antagonists in Marfan syndrome, based on individual patient data: a report from the Marfan Treatment Trialists' Collaboration. Am Heart J 169:605–612

Pyeritz RE (2014) Heritable thoracic aortic disorders. Curr Opin Cardiol 29:97–102

Robertson IB, Rifkin DB (2016) Regulation of the bioavailability of TGF-b and TGF-b-related proteins. Cold Spring Harb Perspect Biol 8(6):a021907

Sakai LY et al (2016) FBN1: the disease-causing gene for Marfan syndrome and other genetic disorders. Gene 591:279–291

van de Laar IM et al (2011) Mutations in SMAD3 cause a syndromic form of aortic aneurysm and dissections with early-onset osteoarthritis. Nat Genet 43:121–126

Wagenseil JE, Mecham RP (2009) Vascular extracellular matrix and arterial mechanics. Physiol Rev 89:957–989